

Development of Multiplexed Immuno-N-Terminomics to Reveal the Landscape of Proteolytic Processing in Early Embryogenesis of *Drosophila melanogaster*

Sanghee Shin, Ji Hye Hong, Yongwoo Na, Mihye Lee, Wei-Jun Qian, V. Narry Kim, and Jong-Seo Kim*



Cite This: *Anal. Chem.* 2020, 92, 4926–4934



Read Online

ACCESS |



Metrics & More

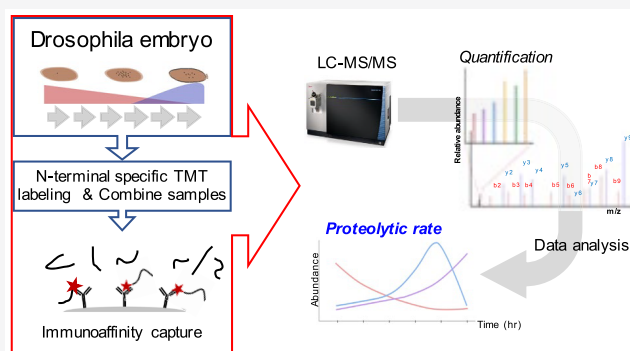


Article Recommendations



Supporting Information

ABSTRACT: Protein expression levels are regulated through both translation and degradation mechanisms. Levels of degradation intermediates, that is, partially degraded proteins, cannot be distinguished from those of intact proteins by global proteomics analysis, which quantify total protein abundance levels. This study aimed to develop a tool for assessing the aspects of degradation regulation via proteolytic processing through a new multiplexed N-terminomics method involving selective isobaric labeling of protein N-termini and immunoaffinity capture of the labeled N-terminal peptides. Our method allows for not only identification of proteolytic cleavage sites, but also highly multiplexed quantification of proteolytic processing. We profiled a number of potential cleavage sites by signal peptidase and provided experimental confirmation of predicted cleavage sites of signal peptide. Furthermore, the present method uniquely represents the landscape of proteomic proteolytic processing rate during early embryogenesis in *Drosophila melanogaster*, revealing the underlying mechanism of stringent decay regulation of zygotically expressed proteins during early stages of embryogenesis.



Protease-mediated proteolytic processing plays a fundamental role in regulating cellular protein levels. In humans, over six hundred proteases are expressed and are responsible for not only protein turnover but also regulation of protein function.^{1–4} Owing to the irreversible nature of proteolytic processing, not only expression but also functional activation of proteases should be strictly regulated in diverse biological phenomena.^{5–8} Despite the functional importance and the numerous proteases encoded by the human genome, the mechanisms underlying proteolytic regulation and protein degradation dynamics in biological phenomena are yet unclear at the system biology level.

To investigate such proteolytic mechanisms and the functional roles of proteases at the proteome level, liquid chromatography and tandem mass spectrometry (LC-MS/MS)-based proteomics approaches targeting proteolytic cleavage sites, that is, both neo C- and N-termini of proteins, have been developed largely through two strategies: first, selective enrichment of the peptides at the proteolytic cleavage site (i.e., C- or N-terminal peptides) via chemical^{9–11} or enzymatic^{12–16} tagging of specific probes including biotin (positive capture); second, depletion of internal peptides (i.e., non N- or C-terminal peptides) via scavenger resins, thus enriching terminal peptides in flow through (negative capture).^{17–20} However, most approaches only identify

proteolytic cleavage sites and are largely not capable of sample multiplexing.

Considering the relatively high run-to-run variation largely originated from serial chemical derivatization and enrichment in N-terminomics approaches, a novel approach with a high order of multiplexity minimizing the experimental variations in the enrichment process is highly desirable. Prudova et al.^{21,22} and Klein et al.²³ introduced isobaric labeling-based N-terminomics methods via negative capture (TAILS) for sample multiplexing, requiring large amounts of isobaric reagents, since all primary aminogroups need to be blocked by the isobaric reagent before digestion. Furthermore, proteolytic cleavage sites could be underrepresented in these negative capture methods since >50% of the captured N-terminal peptides were in vivo blocked peptides such as acetylated N-termini in mammalian cells. Regarding the positive capture approach specifically targeting proteolytic cleavage sites, however, no sample multiplexing method allowing high multiplexity (e.g., ≥ 3) has been proposed thus far.

Received: November 5, 2019

Accepted: March 20, 2020

Published: March 20, 2020



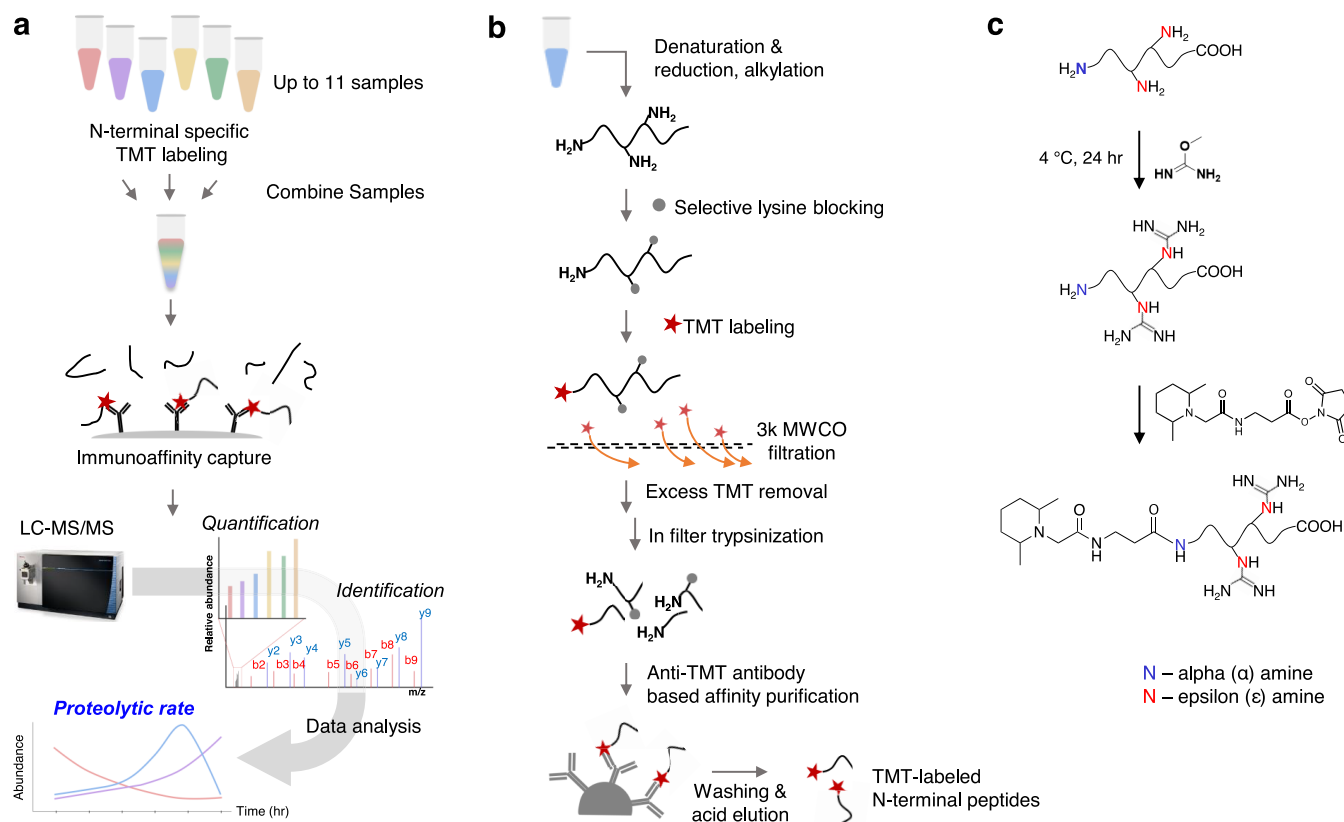


Figure 1. Schematic workflow and detail labeling scheme for the multiplexed immuno-N-terminomics (*miNterm*). (a) Overall strategic scheme of *miNterm* experiment based on the TMT labeling and immunoaffinity capture. (b) A detailed schematic workflow for the chemical labeling and enrichment of N-terminal peptides. (c) N-terminal-specific TMT labeling scheme via guanidination of lysine residues.

Here, we introduce a cost-effective positive capture method for multiplexed N-terminomics (up to 11-plex), enabling not only identification but also highly multiplexed quantification of protein N-termini or proteolytic cleavage sites. Our method is based on the selective blocking of lysine residues and isobaric labeling of protein N-termini with only tandem mass tag (TMT) reagents. TMT-labeled N-terminal peptides can be positively captured via immunoaffinity purification using an immobilized anti-TMT antibody resin. This method was first optimized with regard to both labeling and immunocapture efficiencies using a TMTzero reagent in *Drosophila melanogaster* Schneider 2 (S2) cell lysate, and an experimental annotation approach of signal peptide (SP) cleavage site was proposed based on the differential MS intensity of N-terminal peptides from the S2 samples. To assess the unclear aspects of proteolytic regulation, we applied our multiplexed immuno-N-terminomics (*miNterm*) method using TMT-6plex reagent to *D. melanogaster* early embryos. The result from the normalized *miNterm* by global proteomics data (i.e., presumable proteolytic rate) represented an active landscape of proteolytic dynamics during early development, thus unveiling hidden proteolytic regulation of both maternal and zygotic proteins.

EXPERIMENTAL SECTION

Cell Culture and *Drosophila* Embryo Collection. *D. melanogaster* S2 and Kc167 cells were grown in complete Schneider's *Drosophila* medium supplemented with 10% heat-inactivated fetal bovine serum. *Drosophila* embryo was collected as previously described.²⁴

Protein Extraction and Alkylation of Protein Thiols.

Cells or embryos were lysed using 6 M guanidine-HCl/200 mM HEPES buffer (pH 8.0) containing 1x protease inhibitor cocktail. Protein extract was then denatured by incubating at 37 °C for 1 h. Protein thiols were reduced and alkylated with 10 mM dithiothreitol and 40 mM iodoacetamide, respectively.

TMT-Labeling on Protein N-Termini via Lysine-Selective Blocking Chemistry. To selective blocking of ε-amine in lysine residue, pH of protein extract was adjusted to 10.5 and final 1 M of *o*-methylisourea solution (pH 10.5) was added to the sample and incubated for >24 h at 4 °C with constant rotation. After selective lysine blocking, pH of sample was readjusted to 8.0, and each channel of TMT reagent was added to protein sample at 1.5-fold (w/w) under 33% of acetonitrile condition. After 1 h of incubation for TMT labeling of the N-terminus, 500 mM of hydroxylamine was added to sample to quench the labeling reaction.

Excess TMT Removal and Protein Digestion. Excess TMT reagent was removed by three step filtration using a 3 kDa MWCO filter unit. The buffer was exchanged into 8 M Urea with 20% ACN containing 50 mM ammonium bicarbonate buffer. Then trypsin was added to the filter unit with a 1:50 enzyme to protein ratio (w/w) for in-filter digestion.

Capture of N-Terminal Peptides Using Immobilized Anti-TMT Antibody Resin. The merged peptide sample incubated with immobilized anti-TMT antibody resin with a peptide to resin ratio of 1:2 (w/v) then, incubated for 2 h at room temperature. After incubation, supernatant was discarded, and the resin was washed with following steps: 2 times

with 1× TBS buffer, 2 times with 2 M urea buffer followed by 2 times with 0.1% sodium deoxycholate buffer and finally 3 times with 1× TBS. The captured N-terminal peptides were eluted with 50% ACN in 0.4% trifluoroacetic acid.

LC-MS/MS and Data Analysis. The eluted samples were subjected to desalting prior to LC-MS/MS analysis and finally analyzed on Q-Exactive or Orbitrap Fusion Lumos mass spectrometer. LC-MS/MS data of *miNterm* was searched with Thermo Proteome Discoverer (version 2.3) at 1% FDR at protein level with the following parameters: semitryptic digestion, fixed carbamidomethylation on cysteine, homoarginine modification on lysine residue, TMT modification on peptide N-terminus, and dynamic oxidation on methionine.

RESULTS

Strategy for Selective Isobaric Labeling and Enrichment of Protein N-Termini. Figure 1a provides an overview of our *miNterm* method. Up to 11 samples can be subjected to N-terminal specific TMT-labeling. First, every lysine residue is selectively blocked, while the N-terminal amino group remains intact. Thereafter, protein N-termini are labeled with TMT reagents (Figure 1b,c). To specifically isolate the TMT-labeled N-terminal peptides, immunoaffinity enrichment using the immobilized anti-TMT antibody resin is carried out after trypsinization of the combined multiple samples (Figure 1b). Enriched N-terminal peptides are then analyzed via LC-MS/MS, thus revealing the relative quantities of multiplexed samples as report ion intensities.

To selectively label the protein N-termini with the TMT reagent, the preblocking chemistry of all lysine residues should show a quantitative conversion yield, preserving N-terminal amino groups. The conversion of the lysine amino group to guanidino group was kinetically preferred to N-terminal guanidination at low temperatures such as 4 °C, resulting in selective conversion of lysine to homoarginine with high efficiency, while most N-termini were intact (Figure 1c).^{9,11,25} Thus, we adopted the guanidination reaction and confirmed the high blocking efficiency (98.2%) (Supporting Information (SI) Table S2) and lysine-selectivity of guanidination in that less than 1% of protein N-termini can be guanidinated (SI Table S3).

Optimization of Protein-Level TMT Labeling and Immunoaffinity Capture. Although the TMT labeling protocol has been established at the peptide level, optimal conditions at the protein level may differ from those at the peptide level in terms of reagent molar ratio and buffer composition, where the use of organoaqueous buffer was recommended by manufacturer. We initially checked out the impact of organoaqueous buffer composition on proteome solubility and then optimized the amount of TMT reagent to label standard proteins (BSA, enolase, insulin, α -lactalbumin, RNase A, and GAPDH) using TMTzero reagent. We found up to 40% of ACN organoaqueous buffer can be used without protein precipitation in cell lysate sample (SI Figure S1a) and observed stable TMT-labeling efficiencies in such ACN% range (SI Figure S1b and Table S4). In principle, higher content of organic solvent can be beneficial for protein denaturation and preserving TMT reagent against hydrolysis. Thus, we decided to use 33% of ACN organoaqueous solution for next all experiments. For all six model proteins, highly consistent labeling efficiencies were obtained from triplicate experiments across various TMT doses (SI Figure S1c and Table S5). Intriguingly, a lower level of TMT reagent (150 μ g/

100 μ g protein sample) than that recommended by the manufacturer (800 μ g) seems sufficient to efficiently label the remaining N-terminal amino group in BSA, enolase (SI Figure S1c), and Kc167 cell lysate (SI Figure S1d and Table S6), probably because most primary amino groups, that is, lysine residues, were inactivated after guanidination. However, we observed a large protein-specific variation in TMT-labeling at protein level (SI Figure S1c–e). For some proteins, a much higher dose of TMT reagents seems to be necessary to achieve full labeling (SI Figure S1c). If the N-termini of solidly structured proteins such as lactalbumin^{26,27} and RNase A²⁸ might not be fully exposed to solvent and TMT reagent even after denaturation step, it could result in the inefficient TMT labeling. Given that our method is targeting the proteolytic cleavage sites and the labeling efficiency of digested sample was quite high at the same TMT dose (SI Figure S1f), the proteome-wide TMT-labeling efficiency in endogenously proteolytic processed samples can be higher than that observed in the lysate sample (78%) without enrichment.

Elimination of excess TMT reagent moieties after labeling/quenching is mostly critical for the success of immunoaffinity purification of TMT-labeled N-terminal peptides. Otherwise, the remaining TMT moieties would severely compromise the binding of true peptide targets (i.e., N-terminal peptides). We assessed both acetone precipitation and size cutoff filtration (3 kDa) to determine the respective capability for eliminating excess reagents. The quenched product of TMTzero by hydroxylamine (MH^+ 258.182 Da, SI Figure S2a) was targeted via LC-MS analysis to estimate the amount of remaining TMT reagents after elimination. Based on the extracted chromatographic peak area, three repetitive filtration steps would be necessary and sufficient to eliminate excess TMT moieties, while the acetone precipitation approach showed inferior capability, and the BCA protein assay was severely compromised by the remaining TMT reagent and hydroxylamine (SI Figure S2b,c).

We further examined the impact of such approaches on the overall enrichment of TMT-labeled N-terminal peptides. As a result, it was confirmed that three times filtration is required, resulting in the highest peak areas of N-terminal peptides for all six proteins (SI Figure S2d,e). Intriguingly, when we used less amount of TMT reagents ($1/3$ TMT dose), only twice filtration was sufficient to lead to the second enrichment yield (SI Figure S 2d,e). Taken together, we can conclude that the three times filtration would be required at the optimized TMT dose, while the number of filtration can be reduced when less TMT dose is applied.

Furthermore, we optimized the relative antibody levels and the washing/elution conditions in immunoaffinity purification to minimize nonspecific binding of the supermajority, that is, non-TMT-labeled peptides (SI Figure S3 and Table S7). We generated a HeLa digest spiked with 5% w/w TMT-labeled BSA digest as a mimicked N-terminal TMT-labeled proteome and used it for further optimization. We investigated the ideal ratio of the immunoaffinity resin (μ L) to the peptide sample (μ g) and observed that a 2-fold amount of resin compared to the peptide sample was sufficient to efficiently capture the TMT-labeled peptide, since the captured proportion of TMT-labeled peptides displayed maximum efficiency under specified conditions (SI Figure S3a). Using the same spiked sample, we screened a series of washing conditions (SI Figure S3b) and found that anti-TMT antibody allowed for the use of both 2 M urea and 0.1% sodium deoxycholate as washing solutions, thus

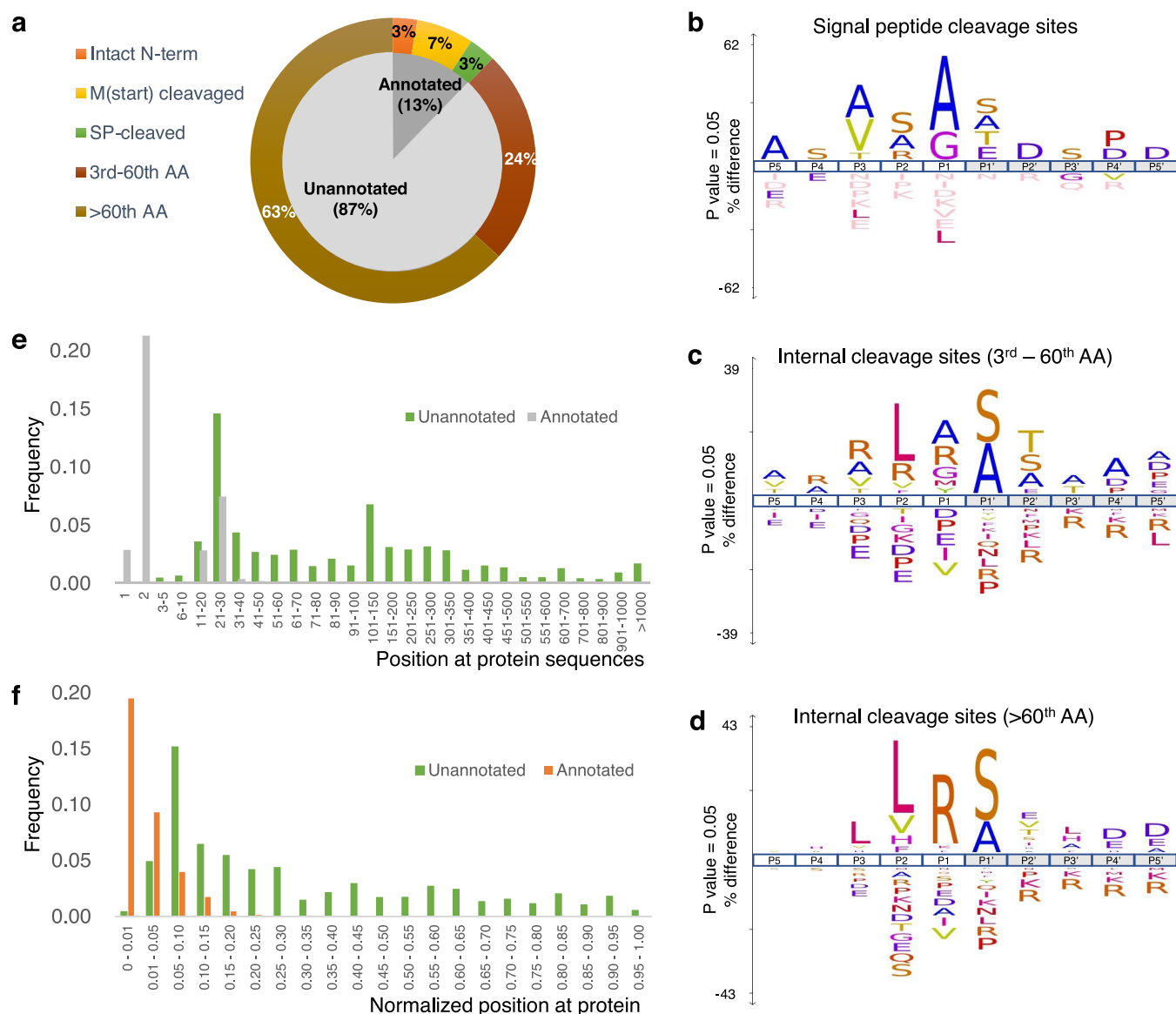


Figure 2. The results of immuno-N-terminomics analysis of S2 cells of *D. melanogaster*. (a) Composition of identified neo-N-termini (P1') from S2 cells. iceLogo analysis of the identified P1' site categorized as the signal/transit peptide (b), internal cleavage sites positioned between the 3rd and 60th amino acid (c), and internal cleavage sites positioned after the 60th amino acid (d). Intensity proportion of identified P1' sites among aligned positions at protein sequences (e) and at normalized protein position (f).

increasing the specificity of TMT-labeled peptides by washing out the nonspecific peptides and simultaneously preserving the affinity for TMT-labeled peptides (SI Figure S3c). Of note, elution with the commercial TMT Elution buffer, containing a TMT-competitor with higher affinity for the antibody, was worse than that with the conventional acidic elution, generating significantly poorer chromatograms for identification of the TMT-labeled peptides (SI Figure S3d,e). We summarized the whole optimized steps in SI Table S1 and applied the optimized protocol to all the following experiments in *D. Melanogaster* samples.

Proteome-Wide Profiling of Protein N-Termini for *D. melanogaster* S2 Cells. To verify the applicability of our method for complex proteome samples, we applied the entire protocol to *D. melanogaster* S2 cells using TMTzero reagent without sample multiplexing at that stage. Biological duplicate experiments were reproducibly carried out, revealing 3095 nonredundant N-terminal peptides and 2825 N-terminal sites

from 1322 proteins at a <1% false discovery rate (FDR) (SI Figure S4a,b and Table S8). The identified N-terminal sites were classified into UniProt-annotated or unannotated sites, which are functionally intact N-terminal sites (e.g., intact N-terminal sites, intact methionine-removed sites, or SP-cleavage sites) or proteolytic processing sites, respectively (Figure 2a). As expected, proteolytic cleavage sites were dominantly enriched (87%) in our positive capture methods. Of note, the iceLogo pattern showing amino acid frequency for the UniProt-annotated SP-cleavage sites (Figure 2b) was clearly different from that for the unannotated N-terminal sites (Figure 2c,d). Furthermore, the iceLogo analysis for unannotated N-terminal sites located at ≤ 60 th amino acid residue in the protein sequence showed different pattern from that for the other part (>60th). The latter showed the strongest enrichment of the arginine residue at position P1, indicating the potential involvement of endogenous Arg-C-like proteases in protein turnover in S2 cells (Figure 2d), while the

former, which potentially can be originated from signal/transit peptide cleavage, represented a little bit mixed pattern of both the annotated one and the latter (Figure 2c), implying that a certain portion of unannotated SP-cleavage sites might be included. Various amino acids encompassed most of the N-terminal sites at the P1 and P1' positions of presumably endogenous proteases (SI Figure S4c), indicating that active proteolytic events occurring in vivo can be successfully captured by the present method.

When we aligned the identified N-terminal sites into position in protein sequences, we found that they were largely well-distributed throughout diverse positions with quantitatively three peak regions proximal to the intact start position, SP-cleavage sites (21–30), and at position 101–150 (Figure 2e). On normalizing the position of N-terminal sites by total protein length, we observed a significant MS signal intensity near the potential signal/transit peptide cleavage sites (0.05–0.10 in normalized position) for unannotated N-terminal sites (Figure 2f), suggesting that these experimentally determined N-terminal sites might represent the unannotated cleavage sites of signal/transit peptides. Furthermore, we found that the internal cleavage sites located over 0.30 in the normalized position were quantitatively balanced in their distribution within the protein (Figure 2f), indicating that proteolytic events occur throughout various regions of the protein in an unbiased manner.

Given that our method bypasses the endogenously blocked N-termini such as acetylated N-termini, corresponding to >50% of the N-termini in mammalian cells, and only targets the free N-terminal sites in vivo, all these results clearly demonstrate that the whole optimized protocol including chemical derivatization and immunoaffinity capture processes in the present method works unbiasedly and effectively to reveal the diverse proteolytic events occurring in complex samples.

Intensity Based Experimental Annotation of SP-Cleavage Sites. SP sequences are short (~20 amino acid residues) and present at the N-terminus of newly synthesized proteins, providing essential information regarding the function of membrane and secretory proteins; thus, experimental annotation of SP-cleavage sites is necessary but challenging.^{29–31}

Intriguingly, we observed several N-terminal sites sequentially located proximal to the UniProt-annotated signal/transit peptide cleavage site in many proteins. We hypothesized that the functionally active SP-cleavage site would be dominant in vivo, thereby representing the strongest MS intensity among the sequential N-terminal sites. To investigate this hypothesis, the intensities of UniProt-annotated SP-cleavage sites and their nearby sites (± 2 amino acids, i.e., P2–P3' sites) identified in this study were normalized by the maximum intensity for each protein, and represented as a heat map (Figure 3a and SI Table S9). Consistent with our hypothesis, the cleavage sites of 99 proteins annotated through the UniProt database (3 from the published literature, 95 by prediction tool without experimental evidence, and 1 N/A) displayed the strongest intensity at the matching site (Group 1 in Figure 3a and SI Figure S5a,b), demonstrating that intensity-based annotation of SP-cleavage site is feasible and thereby provides experimental confirmation for the sites annotated by only prediction analysis (95 proteins in this study). For example, Éclair (*Eca*), an essential protein required for dorsoventral embryonic patterning and involved in Golgi organization,^{32,33} yielded two

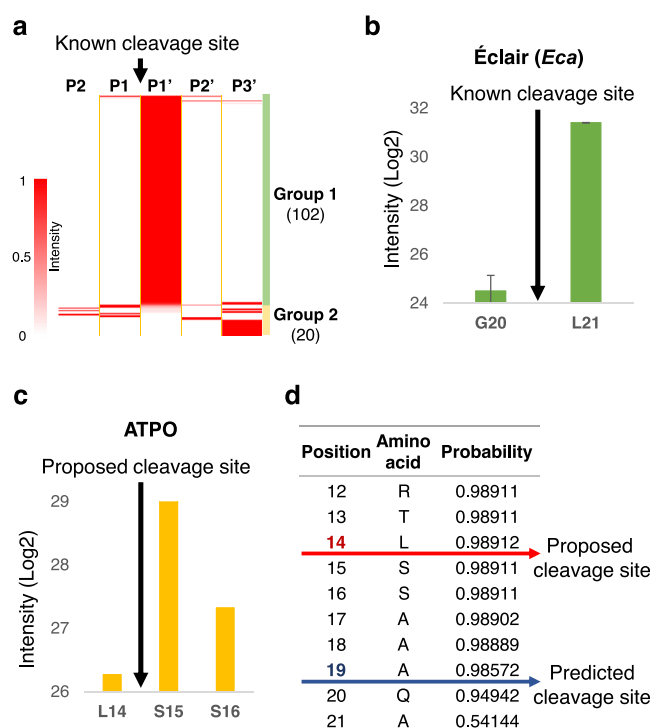


Figure 3. Intensity-based experimental annotation of signal peptide cleavage sites in *D. melanogaster*. (a) The intensity heat map of UniProt-annotated signal/transit peptide cleavage sites and their nearby sites (± 2 amino acids, i.e., P2–P3' sites) identified in this study. The intensities are normalized by the maximum intensity for each protein. Examples of quantity-based annotation of signal peptide cleavage sites among the identified P1' sites: Éclair, consistent with the UniProt-annotation (b) and ATPO, different from predicted site and signal peptide cleavage site newly proposed (c). (d) Signal peptide probability of ATPO predicted by the Phobius tool and predicted and experimentally proposed signal peptide cleavage sites.

continuous neo-N-termini (G20 and L21) wherein the cleavage site inferred from 7-fold stronger N-terminal peptide corresponded to the SP-cleavage site that was UniProt-annotated (Figure 3b) and Phobius-predicted (SI Figure S5c).³⁴ These results indicate that the quantity-based annotation approach could be utilized to discover or reannotate signal/transit cleavage site.

Accordingly, via the aforementioned approach, we investigated the neo-N-terminal sites of 17 proteins (Group 2 in Figure 3a) whose exact SP-cleavage sites are yet unknown or not predicted. For example, the ATP synthase subunit O (ATPO) was identified with three continuous N-terminal sites (L14, S15, and S16) that displayed the highest intensity at S15 with a greater fold change than their neighboring sites, indicating that the C-terminal position L14 is potentially the most probable cleavage site (Figure 3c and SI Table S9). This site is different from the Phobius-predicted site (19th), but still displays a high probability score (Figure 3d). As a result, we could propose a putative SP-cleavage site for the respective 18 proteins including ATPO based on N-terminomics results (SI Table S9).

Multiplexed Immuno-N-Terminomics Reveals Dynamics of Proteolytic Processing during Early Embryonic Development in *D. Melanogaster*. During early embryonic maternal-to-zygotic transition (MZT), a large proportion of maternally pre-existing proteins are degraded,

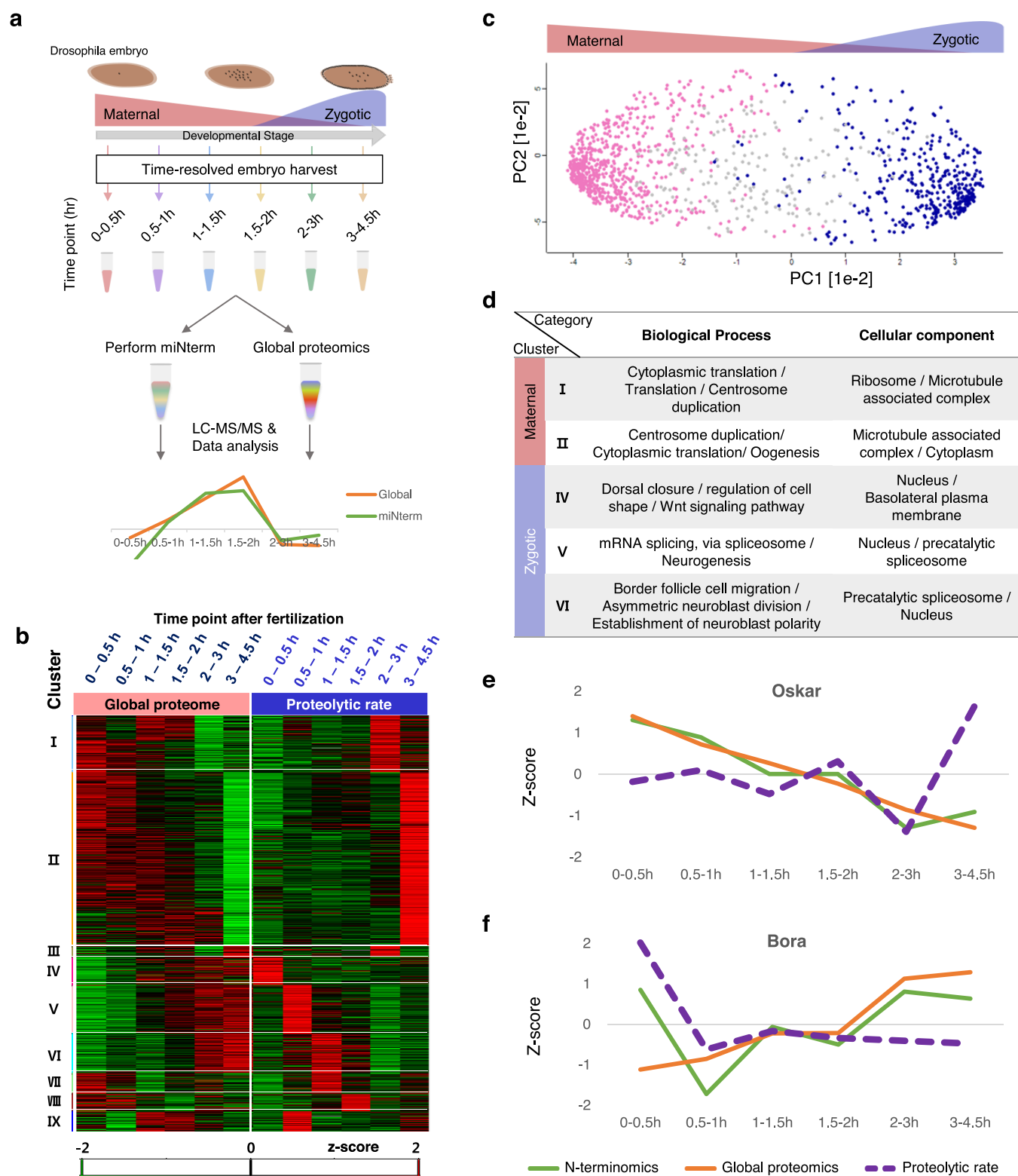


Figure 4. Time-resolved multiplexed immuno-N-terminomics (*miNterm*) and global proteomics profiling during the *Drosophila* maternal-to-zygotic transition (MZT). (a) Schematic representations of *miNterm* and global proteomics experiments performed for *Drosophila* embryos during the maternal-to-zygotic transition (MZT). (b) Heatmap of the global proteome change and degradation rate trend determined through cluster analysis. Z-scores were individually normalized within the degradation rate and global proteome. (c) The principle component analysis clearly differentiated maternal clusters from zygotic clusters; maternal proteins (cluster I–II) colored as pink, zygotic proteins (cluster IV–VI) colored as blue. (d) The representative gene ontology terms of biological processes and cellular for each cluster. Representative temporal trends of the N-terminomics signal, global proteome and the derived degradation rate during embryogenesis of a maternal gene, *Oskar* (e) and a zygotic gene, *Bora* (f).

while zygotically synthesized proteins undertake developmental roles.^{35–38} The decay dynamics of maternally deposited proteome can be obtained with global proteomics experiment; however, that of zygotically translated proteome would not be accessible via the same approach since zygotic protein levels gradually increase in general. Given that our method could quantitatively profile the proteolytic processing products in a multiplexed manner, it could disclose the hidden proteolytic regulation of zygotic as well as maternal proteome during early embryogenesis.

Thus, we carried out a multiplexed version of the present immuno-N-terminomics method with TMT-6plex reagent for time-resolved profiling of protein N-termini in the *D. melanogaster* MZT. *D. melanogaster* early embryos at six different developmental stages were carefully harvested and their respective lysates were individually subjected to N-terminal-selective TMT labeling. The six proteome samples labeled with the respective TMT-6plex reagent were combined and subjected to anti-TMT immunoaffinity capture after trypsinization, followed by LC-MS/MS analysis (Figure 4a). Biological duplicate experiments generated 4,936 nonredundant N-terminal peptides from 1449 protein groups (SI Table S10) with high enrichment specificity (92.5% in spectrum-level, SI Table S11) and reproducibility ($R = 0.893$ in SI Figure S6a). Again the majority of identified N-terminal sites (95%) corresponded to the unannotated N-terminal sites, highlighting proteolytic products with various compositions at P1 and P1' site and proportions at different time points (SI Figure S6b,c). iceLogo analysis was carried out for the identified N-terminal sites and displayed quite different patterns between yolk proteins (SI Figure S6d) and others (SI Figure S6e). The latter pattern showed similarities with cathepsin-like degradation (SI Figure S6e), indicating that cathepsin-like proteases might be primarily involved in proteolytic protein regulation in embryogenesis.^{39–42} Of note, we identified a family of cathepsin proteases such as cathepsin L, cathepsin D and cathepsin B1 in our *miNterm* data (SI Table S10). Also it was reported that maternally provided cathepsin L is essential for the development of *C. elegans* during embryogenesis.⁴³ Furthermore, other serine proteases such as easter and nudel, which are the critical components of the extracellular signaling pathway responsible for the dorsal-ventral pattern formation in early embryogenesis,^{44,45} were identified (SI Table S10). Although the underlying mechanism of how cathepsin family and other proteases regulate the early development have not been fully understood, we hope our data set could facilitate further discovery of the functional mechanism of such cathepsin proteases in embryogenesis.

Of note, the dynamics of the degradome from *miNterm* data can be directly converted to presumable “proteolytic rate” in that biological context by normalizing the *miNterm*-signals by global expression levels at each time point. To this end, we carried out global proteome profiling of *D. melanogaster* MZT based on TMT labeling approach at the specified time points (Figure 4a and SI Table S12). As a result, we derived a trend of protein “proteolytic rate” from the integration of both global proteome and degradome levels: first, we merged the TMT signals of N-terminal sites for respective proteins excluding the annotated N-terminal sites (i.e., internally proteolytic cleavage sites only, SI Figure S6a). Second, the merged signals were normalized by the protein expression levels at the respective time points, deriving trends of proteolytic rate. After clustering analysis, the global abundance changes and trends of

proteolytic rate during MZT were displayed as a heat map comprising nine clusters (Figure 4b and SI Table S12). The clustering analysis showed two major groups, that is, maternally deposited proteins, down-regulated (Cluster I–II), and zygotically translated proteins, up-regulated (Cluster IV–VI). The proteins corresponding to each group clearly represent significantly contrasting pattern to each other in the principal component analysis, indicating their distinctive protein dynamics during the embryogenesis (Figure 4c). The representative gene ontology (GO) terms in biological processes and cellular compartments for the respective cluster were also presented (Figure 4d).

The down-regulated maternal protein clusters (I and II) showed closely related GO terms to mitosis and cytoplasmic transition (Figure 4d), consistent with previous studies reporting that embryos undergo rapid cell proliferation, skipping the gap phases and that cell cycle-regulating mRNAs are depleted until the midblastula transition (MBT) (at 1.5–2 h in this study).^{46,47} The average temporal trend of proteolytic rate in Cluster II was clearly negatively correlated with that of steadily decreasing global expression level (SI Figure S7a), showing that maternally translated proteins are actively degraded after MBT along with maternal mRNAs. Intriguingly, the proteolytic rate of *Oskar* in Cluster II, which is a maternal effect gene helping the localization of proteins and RNAs required at the posterior pole of the embryo,^{48,49} slightly bounced up right after MBT and steeply up-regulated in late time point, while the global expression level was gradually depleted (Figure 4d), indicating that an active decay regulation might be programmed for this protein shortly after MBT. These results show how *miNterm* could be utilized for discovery of hidden decay regulations even for down-regulated proteins.

On the other hand, the zygotic protein clusters (IV–VI) were clearly up-regulated in agreement with the fact that these gene products direct further embryonic development after MBT. Most intriguingly, the average proteolytic rate of cluster IV was significantly up-regulated at very early time point and maintained at a constant level after rapid reduction passing through MBT (SI Figure S7b). For example, *Bora* (Figure 4e) and *BRWD3* (SI Figure S7c), which are responsible for cell fate determination⁵⁰ or cell differentiation,^{51,52} respectively, showed considerable *miNterm* signals and corresponding high proteolytic rates at the very early stage of development. Given that the mRNA levels of these genes are very low in that early phase⁵³ (SI Figure S7d), these results indicate that a certain amount of these proteins might be maternally deposited and subsequently subjected to rapid proteolytic clearance at the early time point to keep them at basal level. Collectively, all these results illustrate that our multiplexed version of immuno-N-terminomics method is quite useful to disclose trends of proteolytic rate and undiscovered decay regulation in cellular events.

DISCUSSION

We developed a multiplexed N-terminomics method via immunoaffinity capture, which enables not only highly selective enrichment of N-terminal peptides of proteins but also facilitates highly multiplexed profiling of proteolytic processing through multiple time points for up to 11 samples. The nature of isobaric labeling in the *miNterm* method, that is, enhancing precursor ion intensity by merging peptide signals from multiplexed samples, is highly beneficial for the detection of transient and low-abundant proteolytic intermediates.

Furthermore, the present 6-plex *miNterm* data are the first comprehensive *in vivo* data set for *Drosophila* MZT degradomics, encompassing multiple developmental stages of embryogenesis.

Given that not only protein translation but also protein decay modulates protein expression level, the landscape of decay regulation at the system-wide level is not well represented so far, mainly owing to the lack of suitable omics tools, whereas protein translation has been assessed with various omics approaches indirectly (mRNA-seq/ribosome profiling) or directly (pulsed SILAC). For example, the proteomic investigation of decay regulation has relied on the measurement of proteome change between different steady-states (i.e., global proteomics); however, global proteomics data could not distinguish degradation intermediates from intact proteins and never represent proteolytic events in up-regulated proteins, thereby providing limited or biased information for protein decay. As aforementioned, our *miNterm* method allows for comprehensive profiling of proteolytic intermediates and generates proteolytic dynamics via normalization by global proteomics data for a given biological event. The capability to catch the degradome and to reveal the decay dynamics can facilitate novel findings of proteolytic regulation in a variety of biological and clinical samples.

It should be noted that not all proteolytic intermediates are generated by a manner of degradation process. Indeed, many mature functional proteins are actually posttranslational proteolytic products during the maturation process (e.g., insulin⁵⁴ or caspases⁵⁵). Hence it is inaccurate to affirm the merged N-terminal signals as degradation dynamics. To avoid potential misinterpretation, we excluded the annotated N-terminal sites in the dynamics of proteolytic rate. We observed that the unannotated, 95% of proteolytic cleavage sites in embryo sample spread throughout the whole range of proteins (SI Figure S6b) and the dynamics of proteolytic rate for many of well-known maternal proteins showed largely well-matched pattern with global proteome change of them. These results indicate that the major proportion of proteolytic cleavage sites in embryo sample might be originated from the proteolytic processing for protein decay and the impacts of uncharacterized functional N-terminal sites on the dynamics of proteolytic rate might be quite minor.

A drawback in our method would be the overall long sample preparation time largely owing to the selective blocking of lysine amino groups (24 h) and a series of buffer exchange steps for the removal of excess TMT-moiety. However, the one-day time gap makes time-managing easy and does not negatively affect the overall throughput too much. Moreover, the immunoaffinity capture system for N-terminal peptides is far more biology-friendly than the use of chemically functionalized resins such as amine-reactive scavenging resin.

In conclusion, we believe that our *miNterm* analysis serves as a robust platform to assess protein proteolytic processing to elucidate undiscovered decay regulation, which would not be apparent through global proteomics experiment, or to discover biomarkers for diseases related to hyper-activation of proteases such as cancer.

■ ASSOCIATED CONTENT

SI Supporting Information

The Supporting Information is available free of charge at <https://pubs.acs.org/doi/10.1021/acs.analchem.9b05035>.

Whole experimental methods, seven supplementary figures, and seven supplementary tables (PDF)

Table S7 (XLSX)

Table S8 (XLSX)

Table S9 (XLSX)

Table S10 (XLSX)

Table S12 (XLSX)

■ AUTHOR INFORMATION

Corresponding Author

Jong-Seo Kim – Center for RNA Research, Institute for Basic Science, Seoul 08826, Korea; School of Biological Sciences, Seoul National University, Seoul 08826, Korea; orcid.org/0000-0002-8909-8440; Email: jongseokim@snu.ac.kr

Authors

Sanghee Shin – Center for RNA Research, Institute for Basic Science, Seoul 08826, Korea; School of Biological Sciences, Seoul National University, Seoul 08826, Korea

Ji Hye Hong – Center for RNA Research, Institute for Basic Science, Seoul 08826, Korea; School of Biological Sciences, Seoul National University, Seoul 08826, Korea

Yongwoo Na – Center for RNA Research, Institute for Basic Science, Seoul 08826, Korea; School of Biological Sciences, Seoul National University, Seoul 08826, Korea

Mihye Lee – Soonchunhyang Institute of Medi-bio Science, Soonchunhyang University, Cheonan-si, Chungcheongnam-do 31151, Korea; orcid.org/0000-0001-9689-6937

Wei-Jun Qian – Integrative Omics, Biological Sciences Division, Pacific Northwest National Laboratory, Richland, Washington 99352, United States; orcid.org/0000-0002-5393-2827

V. Narry Kim – Center for RNA Research, Institute for Basic Science, Seoul 08826, Korea; School of Biological Sciences, Seoul National University, Seoul 08826, Korea

Complete contact information is available at: <https://pubs.acs.org/doi/10.1021/acs.analchem.9b05035>

Author Contributions

J.-S.K. and W.-J.Q. conceived the concept of multiplexed N-terminomics. J.-S.K. designed experiments and supervised the project. S.S. and J.H.H. carried out protocol development and proteomics experiments with the support of Y.N. and M.L. V.N.K. provided all experimental resources. S.S. and J.-S.K. wrote the manuscript with help of all other authors.

Notes

The authors declare no competing financial interest.

■ ACKNOWLEDGMENTS

This work was supported by the fund from Institute for Basic Science of Korea (IBS-R008-D1) and by the BK21 Research Fellowships from the Ministry of Education of Korea (S.S., Y.N.).

■ REFERENCES

- (1) Puente, X. S.; Sánchez, L. M.; Overall, C. M.; López-Otín, C. *Nat. Rev. Genet.* **2003**, *4*, 544.
- (2) Fujinaga, M.; Cherney, M. M.; Oyama, H.; Oda, K.; James, M. N. G. *Proc. Natl. Acad. Sci. U. S. A.* **2004**, *101* (10), 3364.
- (3) Ciechanover, A. *Nat. Rev. Mol. Cell Biol.* **2005**, *6* (1), 79–87.
- (4) López-Otín, C.; Bond, J. S. *J. Biol. Chem.* **2008**, *283* (45), 30433–30437.
- (5) López-Otín, C.; Overall, C. M. *Nat. Rev. Mol. Cell Biol.* **2002**, *3*, 509.

- (6) Selkoe, D.; Kopan, R. *Annu. Rev. Neurosci.* **2003**, *26* (1), 565–597.
- (7) Bai, G.; Pfaff, S. L. *Neuron* **2011**, *72* (1), 9–21.
- (8) Lomate, P. R.; Dewangan, V.; Mahajan, N. S.; Kumar, Y.; Kulkarni, A.; Wang, L.; Saxena, S.; Gupta, V. S.; Giri, A. P. *Mol. Cell. Proteomics* **2018**, *17* (7), 1324.
- (9) Timmer, J. C.; Enoksson, M.; Wildfang, E.; Zhu, W.; Igarashi, Y.; Denault, J.-B.; Ma, Y.; Dummitt, B.; Chang, Y.-H.; Mast, A. E.; Eroshkin, A.; Smith, J. W.; Tao, W. A.; Salvesen, G. S. *Biochem. J.* **2007**, *407* (1), 41–48.
- (10) Xu, G.; Shin, S. B. Y.; Jaffrey, S. R. *Proc. Natl. Acad. Sci. U. S. A.* **2009**, *106* (46), 19310.
- (11) Kim, J.-S.; Dai, Z.; Aryal, U. K.; Moore, R. J.; Camp, D. G.; Baker, S. E.; Smith, R. D.; Qian, W.-J. *Anal. Chem.* **2013**, *85* (14), 6826–6832.
- (12) Mahrus, S.; Trinidad, J. C.; Barkan, D. T.; Sali, A.; Burlingame, A. L.; Wells, J. A. *Cell* **2008**, *134* (5), 866–876.
- (13) Wildes, D.; Wells, J. A. *Proc. Natl. Acad. Sci. U. S. A.* **2010**, *107* (10), 4561.
- (14) Xu, G.; Shin, S. B. Y.; Jaffrey, S. R. *ACS Chem. Biol.* **2011**, *6* (10), 1015–1020.
- (15) Wiita, A. P.; Hsu, G. W.; Lu, C. M.; Esensten, J. H.; Wells, J. A. *Proc. Natl. Acad. Sci. U. S. A.* **2014**, *111* (21), 7594–7599.
- (16) Calvo, S. E.; Julien, O.; Clauser, K. R.; Shen, H.; Kamer, K. J.; Wells, J. A.; Mootha, V. K. *Mol. Cell. Proteomics* **2017**, *16* (4), 512–523.
- (17) Zhang, X.; Ye, J.; Højrup, P. *J. Proteomics* **2009**, *73* (2), 240–251.
- (18) Kleifeld, O.; Doucet, A.; auf dem Keller, U.; Prudova, A.; Schilling, O.; Kainthan, R. K.; Starr, A. E.; Foster, L. J.; Kizhakkeedathu, J. N.; Overall, C. M. *Nat. Biotechnol.* **2010**, *28*, 281.
- (19) Schilling, O.; Barré, O.; Huesgen, P. F.; Overall, C. M. *Nat. Methods* **2010**, *7*, 508.
- (20) Yeom, J.; Ju, S.; Choi, Y.; Paek, E.; Lee, C. *Sci. Rep.* **2017**, *7* (1), 6599.
- (21) Prudova, A.; auf dem Keller, U.; Butler, G. S.; Overall, C. M. *Mol. Cell. Proteomics* **2010**, *9* (5), 894.
- (22) Prudova, A.; Gocheva, V.; auf dem Keller, U.; Eckhard, U.; Olson, O. C.; Akkari, L.; Butler, G. S.; Fortelny, N.; Lange, P. F.; Mark, J. C.; Joyce, J. A.; Overall, C. M. *Cell Rep.* **2016**, *16* (6), 1762–1773.
- (23) Klein, T.; Fung, S.-Y.; Renner, F.; Blank, M. A.; Dufour, A.; Kang, S.; Bolger-Munro, M.; Scurll, J. M.; Priatel, J. J.; Schweigler, P.; Melkko, S.; Gold, M. R.; Viner, R. I.; Régnier, C. H.; Turvey, S. E.; Overall, C. M. *Nat. Commun.* **2015**, *6*, 8777.
- (24) Lim, J.; Lee, M.; Son, A.; Chang, H.; Kim, V. N. *Genes Dev.* **2016**, *30* (14), 1671–1682.
- (25) Enoksson, M.; Li, J.; Ivancic, M. M.; Timmer, J. C.; Wildfang, E.; Eroshkin, A.; Salvesen, G. S.; Tao, W. A. *J. Proteome Res.* **2007**, *6* (7), 2850–2858.
- (26) Permyakov, E. A.; Berliner, L. J. *FEBS Lett.* **2000**, *473* (3), 269–274.
- (27) Wehbi, Z.; Pérez, M.-D.; Sánchez, L.; Pocióvi, C.; Barbana, C.; Calvo, M. *J. Agric. Food Chem.* **2005**, *53* (25), 9730–9736.
- (28) Yang, H. J.; Tsou, C. L. *Biochem. J.* **1995**, *305* ((Pt 2) (Pt 2)), 379–384.
- (29) Evans, E. A.; Gilmore, R.; Blobel, G. *Proc. Natl. Acad. Sci. U. S. A.* **1986**, *83* (3), 581.
- (30) Li, M.; Zhong, Z.; Zhu, J.; Xiang, D.; Dai, N.; Cao, X.; Qing, Y.; Yang, Z.; Xie, J.; Li, Z.; Baugh, L.; Wang, G.; Wang, D. *J. Biol. Chem.* **2010**, *285* (20), 14871–14881.
- (31) Wang, S.; Wang, D.; Li, J.; Huang, T.; Cai, Y.-D. *Molecular Omics* **2018**, *14* (1), 64–73.
- (32) Bartoszewski, S.; Luschnig, S.; Desjeux, I.; Grosshans, J.; Nüsslein-Volhard, C. *Mech. Dev.* **2004**, *121* (10), 1259–1273.
- (33) Kondylis, V.; Tang, Y.; Fuchs, F.; Boutros, M.; Rabouille, C. *PLoS One* **2011**, *6* (2), No. e17173.
- (34) Krogh, A.; Sonnhammer, E. L. L.; Käll, L. *Nucleic Acids Res.* **2007**, *35* (suppl_2), W429–W432.
- (35) Schier, A. F. *Science* **2007**, *316* (5823), 406.
- (36) Tadros, W.; Westwood, J. T.; Lipshitz, H. D. *Dev. Cell* **2007**, *12* (6), 847–849.
- (37) Benoit, B.; He, C. H.; Zhang, F.; Votruba, S. M.; Tadros, W.; Westwood, J. T.; Smibert, C. A.; Lipshitz, H. D.; Theurkauf, W. E. *Development* **2009**, *136* (6), 923.
- (38) Casas-Vila, N.; Bluhm, A.; Sayols, S.; Dinges, N.; Dejung, M.; Altenhein, T.; Kappei, D.; Altenhein, B.; Roignant, J.-Y.; Butter, F. *Genome Res.* **2017**, *27* (7), 1273–1285.
- (39) Medina, M.; León, P.; Vallejo, C. G. *Arch. Biochem. Biophys.* **1988**, *263* (2), 355–363.
- (40) Kuhn, H.; Sopko, R.; Coughlin, M.; Perrimon, N.; Mitchison, T. *Development* **2015**, *142* (22), 3869.
- (41) Vidmar, R.; Vizovišek, M.; Turk, D.; Turk, B.; Fonović, M. *EMBO J.* **2017**, *36* (16), 2455.
- (42) Schneidman-Duhovny, D.; Khuri, N.; Dong, G. Q.; Winter, M. B.; Shifrut, E.; Friedman, N.; Craik, C. S.; Pratt, K. P.; Paz, P.; Aswad, F.; Sali, A. *PLoS One* **2018**, *13* (11), No. e0206654.
- (43) Britton, C.; Murray, L. J. *Cell Sci.* **2004**, *117* (21), 5133.
- (44) Hong, C. C.; Hashimoto, C. *Cell* **1995**, *82* (5), 785–794.
- (45) Misra, S.; Hecht, P.; Maeda, R.; Anderson, K. V. *Development* **1998**, *125* (7), 1261–1267.
- (46) Langley, A. R.; Smith, J. C.; Stemple, D. L.; Harvey, S. A. *Development* **2014**, *141* (20), 3834.
- (47) Yuan, K.; Seller, C. A.; Shermoen, A. W.; O’Farrell, P. H. *Trends Genet.* **2016**, *32* (8), 496–507.
- (48) Wilhelm, J. E.; Hilton, M.; Amos, Q.; Henzel, W. J. *J. Cell Biol.* **2003**, *163* (6), 1197–1204.
- (49) Kim-Ha, J.; Kerr, K.; Macdonald, P. M. *Cell* **1995**, *81* (3), 403–412.
- (50) Hutterer, A.; Berdnik, D.; Wirtz-Peitz, F.; Žigman, M.; Schleiffer, A.; Knoblich, J. A. *Dev. Cell* **2006**, *11* (2), 147–157.
- (51) Müller, P.; Kutteneuler, D.; Gesellchen, V.; Zeidler, M. P.; Boutros, M. *Nature* **2005**, *436* (7052), 871–875.
- (52) D’Costa, A.; Reifegerste, R.; Sierra, S.; Moses, K. *Mech. Dev.* **2006**, *123* (8), 591–604.
- (53) Becker, K.; Bluhm, A.; Casas-Vila, N.; Dinges, N.; Dejung, M.; Sayols, S.; Kreutz, C.; Roignant, J.-Y.; Butter, F.; Legewie, S. *Nat. Commun.* **2018**, *9* (1), 4970.
- (54) Steiner, D. F.; Oyer, P. E. *Proc. Natl. Acad. Sci. U. S. A.* **1967**, *57* (2), 473.
- (55) Riedl, S. J.; Shi, Y. *Nat. Rev. Mol. Cell Biol.* **2004**, *5* (11), 897–907.